Material-balanced Fischer Assay work (18) was used as a reference point in deriving stoichiometries. The maximum possible oil yield was chosen to be 111% of Fischer Assay based on fluidized-bed pyrolysis results (3, 10).

TABLE I

CHEMICAL REACTION AND RATE EXPRESSIONS THAT DEFINE THE MODEL

Reaction	Rate Expression[a]

Release of Mineral Water[b]
W (bound H_2O) $\rightarrow H_2O(g)$

$$R = k_w W \left[1 - \frac{P_{H_2O}}{P_{eq}} \left(\frac{P_o}{P_t} \right) \right]^8 \quad ; P_{eq} = 4.2 \times 10^{10} e^{-5033/T}$$

$$k_w = 3 \times 10^{48} e^{-(62000 \pm 12400)/T}$$

Kerogen Pyrolysis and Bitumen
$100CH_{1.50}N_{0.025}O_{0.05} \rightarrow 5.3CH_{1.56}N_{0.021}O_{0.01}$ Initial Oil (bitumen)

$+ 74.2CH_{1.56}N_{0.021}O_{0.01}$ $\begin{cases} 10\% \text{ by } k_b = 1 \times 10^{13} e^{-(25160 \pm 1760)/T} \\ 90\% \text{ by } k_o = 2.8 \times 10^{13} e^{-26390/T} \end{cases}$

$+ 14.7CH_{0.63}N_{0.056}O_{0.02}$

$+ 0.3CO + 1.0H_2O$ k_o = above

$+ 0.6CH_4$

$+ 3.6CH_x$ $k_x = 3.3 \times 10^9 e^{-20690/T}$

$+ 1.0H_2$ $k_n = 3.1 \times 10^{13} e^{-27540/T}$

$+ 1.3CO_2$ $\begin{cases} 2/3 \text{ by } k_b = \text{above,} \\ 1/3 \text{ by } k_a = 1 \times 10^{13} e^{-(22000 \pm 2200)/T} \end{cases}$

Oil Vaporization
$Oil_i(\ell) \rightarrow Oil_i(g)$ Fast first-order to Raoult's Law Equilibrium

Oil Coking
$100CH_{0.99}N_{0.038}O_{0.01} \rightarrow 95CH_{0.63}N_{0.04}O_{0.01}$
$+ 3CH_4 + 11H_2 + 2CH_x$ $k_{\ell} = 5.4 \times 10^9 e^{-17620/T}$

Oil Cracking
$Oil_i \rightarrow Oil_{j<i} + char + gases$ (see text) $k_{c,i} = A_i \cdot 1.7 \times 10^6 d^{-19590/T}$

Secondary Char Pyrolysis
$100CH_{0.63}N_{0.05}O_{0.01} \rightarrow 94.5CH_{0.23}N_{0.03}O_{0.01}$
$+ 5.5CH_4 + 6.4H_2 + (2.2NH_3)$ $k_s = 3.3 \times 10^9 e^{-(23210 \pm 2285)/T}$

Tertiary Char Pyrolysis
$100CH_{0.23}N_{0.03}O_{0.01} \rightarrow 100CH_{0.1}N_{0.03}O_{0.01} + 8.0H_2$ $k_t = 3.1 \times 10^{13} e^{-(39000 \pm 4090)/T}$

Dolomite Decomposition
$MgCa(CO_3)_2 \rightarrow MgO + CaCO_3$ $k_d = 2.5 \times 10^{10} e^{-29090/T}$

a. First-order reaction unless otherwise noted. Activation energies with ±values use distributed activation energy theory (17). All rate constants in s^{-1}.
b. P_o (standard), P_t (total), P_{H_2O} and P_{eq} pressures in Pa.
Note: All are converted to a mass basis for the computer code so oil and char compositions are not included explicitly.

TABLE II

PROPERTIES OF THE 11 OIL FRACTIONS

Fraction No.	Average Mol Wt (g/mol)	Average Normal Boiling Point (°C)	Wt % of Bitumen	Initial Wt % of Shale Oil	Wt % of Oil Cokable	Relative Rate of Cracking (A_i)	Antoine Coeffs $\log P = A - B/(T-C)$		
							A(Pa)	B(Pa)	C(K)
1	86	69	0.0	3.85	3.9	1.0	20.725	2696.8	48.8
2	114	126	0.0	5.10	11.8	2.1	20.824	3113.1	64.0
3	142	174	0.7	6.73	19.7	3.8	20.881	3442.8	79.3
4	177	226	5.0	7.69	25.6	6.5	21.017	3833.8	95.2
5	212	271	16.0	8.65	29.6	10.0	21.065	4121.6	111.8
6	261	323	20.3	10.10	33.5	15.8	21.031	4406.2	132.7
7	317	374	10.8	10.58	37.4	24.2	21.213	4763.4	155.7
8	380	422	10.2	12.40	43.4	35.4	21.276	5039.2	178.4
9	464	476	14.7	14.23	47.3	53.8	21.343	5329.1	205.9
10	562	525	13.0	12.02	51.3	80.8	21.400	5577.6	233.1
11	703	594	9.3	8.65	55.2	153.8	21.494	5917.6	273.0

To derive the rate expressions for oil coking, we attempted to mimic the reactions shown in Table I, in that the oil that cokes ($CH_{0.99}N_{0.038}O_{0.01}$) is more aromatic and high in nitrogen content than the average oil ($CH_{1.56}N_{0.021}O_{0.01}$). It was, therefore, assumed that only part of the oil, related to the ^{13}C NMR aromaticity, could coke. The relative amount of each oil fraction that could coke (shown in Table II) was then determined from the relative nitrogen contents. It is well known that the cracking rates of aliphatic compounds depend on their molecular weight. The relative rates, A_i, for cracking of the various oil fractions were calculated from the equation of Voge and Good (19). The preexponential factor was multiplied by a pressure-dependent factor derived from results given by Fabuss (20). The formalism for treating multicomponent oil cracking is then the same as used previously (10). Each of the oil fractions independently undergoes a first-order cracking reaction to generate coke, gas (CO, H_2, CH_4 and CH_x) and lighter oil such that

$$\frac{dy_i}{dt} = \sum_{j=1}^{11} a_{ij} k_{c,j} y_j$$

where

y_i = the weight fraction of the ith oil species

$k_{c,j}$ = the first-order rate coefficient for cracking j^{th} oil species

A_j = relative cracking rate of the jth oil species,

and the stoichiometry factors are:

$a_{ij} = -1$ for i = j

$a_{ij} = 0$ for i > j

and

$a_{ij} = 1/(j + 2.8)$ for i < j

The latter stoichiometry factor is obtained by assuming that equal masses of each of the lighter oil fractions are created by cracking a heavier fraction (approximately true for Voge and Good's data (19)) and that the cracking products are always in the following relative mass ratio with respect to the gas product CH_x: coke, 0.632; CO, 0.0566; H_2, 0.0314; CH_4, 0.166; and Oil_i, 0.50.

The rate parameters for oil degradation could not be used directly because of a lack of data or a difference in formulation of the reactions. The activation energy for shale oil cracking was that determined (10) using an 11-component model for data between 500 and 650°C. The activation energy for oil coking was taken from Campbell et al. (7). The preexponential factors were then adjusted to give agreement with the experimental results of Burnham and Singleton (12), whose

measurements span the largest range of pyrolysis conditions. A close interplay was observed between coking and cracking. That is, reducing the coking rate coefficient caused a decrease in the amount of oil coked, but a nearly compensating increase occurred in the amount of oil cracked. This may be due to a decrease in the flux of sweep gas generated by the coking reaction, thus giving the oil a greater residence time for cracking to occur. The relative amounts of coking and cracking were adjusted using the estimation from oil biomarker content (12) that less than 5% of the oil yield loss at atmospheric pressure and about 10% of the oil yield loss at 2.7 MPA was due to oil cracking. Future experiments at variable porosity will be used to better decouple the liquid and vapor residence times, thereby helping to separate the relative contributions of coking and cracking. The amount of H_2 and CH_4 formed by oil coking was determined from previous data (7), but unlike the original work, we made a correction for the additional H_2 and CH_4 formed at slow heating rates by char pyrolysis.

RESULTS

We first developed an expression for the rate of water release because it has a large impact on the residence time of the generated oil. Our kinetic expression incorporates an equilibrium limitation for clay dehydration. A comparison between calculated time-dependent water production with the measurements of Burnham and Singleton (12) is shown in Figure 1. The agreement is excellent. Although the inhibition of clay dehydration by water vapor is well known (21-22), no suitable kinetics were available for illite, the principal clay in oil shale. Because our rate expression was derived empirically, caution should be used in applying it for pressures and heating rates much outside the range shown in Figure 1.

In Table III, we compare the oil yields calculated by our model with the experimental results of Burnham and Singleton (12). The yields agree very well except at the two extremes of pyrolysis conditions. It would have been possible to fit any subgroup more accurately by sacrificing agreement with the other experiments, but our objective was to see how general a pyrolysis model could be developed. The amount of oil degradation by each mechanism is also shown in Table III. In agreement with previous observations, most of the yield loss at atmospheric pressure is due to oil coking. Both coking and cracking become greater at 2.7 MPa because of longer liquid and gas residence times. Cracking becomes more important at higher pressures. Both oil liquid and oil vapor were allowed to crack, but most of the cracking was calculated to occur in the liquid, perhaps due to the greater mass concentration of the liquid oil compared with the oil vapor.

TABLE III

COMPARISON OF MODEL CALCULATIONS WITH DATA OF BURNHAM AND SINGLETON (12)

Heating Rate (°C/h)	Pressure (MPa)	Oil Yield, Wt % FA		Calculated Yield Loss	
		meas	calc	Coking	Cracking
720	0.1	100	106	5	0.1
110	0.15	97	100	11	0.2
11	0.15	86	89	21	1
1	0.15	77	79	29	3
108	2.7	78	81	22	8
9	2.7	73	70	28	13
1	2.7	72	62	33	16

Note: The maximum calculated oil yield is 111% FA.

Further comparisons of model calculations and measurements of Burnham and Singleton demonstrate the ability of the model to calculate accurately even some properties not used in developing the model. The agreement between observed and calculated oil evolution versus temperature shown in Figure 2 is very good. Most of the delay of oil evolution at increased pressure is predicted using our treatment of oil evaporation. The model has the capability of calculating the change in boiling point properties of the product oil as shown in Table IV. The agreement between observed and calculated gas evolution versus temperature shown in Figure 3 is also very good for the two experiments where data are available. As shown in Table V, the total amounts of H_2, CH_4 and CH_x agree well for the near-atmospheric pressure cases, but significant discrepancies exist for the 2.7 MPa cases, especially for H_2. These discrepancies are discussed in the next section.

We next compare our model calculations with the experiments of Stout et al. (6). These comparisons are especially significant because of the complicated temperature history of the experiments and because no comparisons were made during model development. In these

experiments, the oil shale was heated at 12°C/min to a preselected temperature between 250 and 450°C, held there for either 8, 80 or 800 h, then heated the rest of the way to 500°C at 12°C/min, as shown schematically in Figure 4a. A comparison of measured and calculated yields for these conditions is shown in Figure 4b. We represent the data by lines and the calculations by points because there were more experimental points than model calculations. The lines shown are those drawn by Stout et al. The experiments show that holding at about 350°C is the most sensitive for causing yield loss and that most of the yield loss is caused within 80 h. The model calculations reproduce these features. The model can also reproduce the reported gas compositions as shown in Figure 5.

TABLE IV

COMPARISON OF BOILING POINT DISTRIBUTIONS WITH DATA OF BURNHAM AND SINGLETON (12)

Boiling Interval °C	Fischer Assay		1°C/h, 0.15 MPa		1°C/h, 2.7 MPa	
	exp	calc	exp	calc	exp	calc
<100	4.1	3.8	5.6	6.0	6.9	12.9
100-150	4.4	5.0	5.8	7.6	10.2	14.5
150-200	7.3	6.7	9.7	9.7	14.5	16.3
200-250	8.8	7.9	12.7	11.2	16.3	16.5[a]
250-300	10.8	9.6	16.5[a]	13.0	17.2[a]	16.2
300-350	12.7	11.3	16.3	14.0[a]	15.3	13.0
350-400	13.0	11.1	13.9	12.0	10.6	6.8
400-450	14.4[a]	12.8	11.7	11.4	6.0	2.9
450-500	13.7	14.0[a]	5.8	10.1	2.5	0.7
500-550	8.0	11.0	2.0	4.6	0.5	0.1
>550	2.8	6.8	0.0	0.4	0.0	0.0

a. The most abundant oil fraction.

TABLE V

COMPARISON OF CALCULATED GAS PRODUCTION WITH MEASUREMENTS OF BURNHAM AND SINGLETON (12), IN UNITS OF MMOLE/kg

Heating Rate (°C/h)	Pressure (MPa)	H_2		CH_4		CH_x	
		meas	calc	meas	calc	meas	calc
720	0.1	160	175	107	100	111	109
110	0.15	220	207	127	106	105	112
11	0.15	324	353	184	182	134	125
1	0.15	366	508	205	267	121	147
108	2.7	127	317	252	154	159	183
9	2.7	91	482	374	250	160	249
1	2.7	43	632	312	343	93	294

The final comparisons presented are with experiments involving a gas sweep. Campbell et al. (7) showed that an inert gas sweep could reduce oil yield loss due to coking at low heating rates by increasing the rate of oil vaporization. A comparison between the calculated and observed effect of a gas sweep is shown in Figure 6. Although the general trend is correct, the calculation overestimates the effect. The principal reason is undoubtedly that the experiments have diffusion effects that the model does not take into account, even though the particle size used by Campbell et al. was small (<0.84 mm). A related problem is that the model calculates the same oil yield for Fischer Assay conditions and for pyrolysis at 500°C in a gas sweep. Although evidence is not unanimous (4), it appears most likely that the latter conditions produce 5 to 10% more oil (3, 10). It appears that the model has some problem in calculating the rate of degradation of the 10% most unstable oil. Finally, Herskowitz et al. (11) reported oil yields for pyrolysis of shale heated at 360°C/h and 2.6 Mpa in rapidly flowing N_2 and H_2. They obtained 90% of Fischer Assay yield in N_2 and 117% in H_2. Using the same flowrates as in the experiments, the model calculated oil yields of 106% and 110%, respectively, of Fischer Assay yield. For comparison, the model calculated 106% of Fischer Assay yield at Fischer Assay pyrolysis conditions as shown in Table III. Apparently, the N_2 sweep in the experiments was not capable of completely counteracting the inhibiting effect of

pressure on oil evaporation because of intraparticle diffusion. The difference between experiment and calculation in H_2 indicates that the model does not yet account for all the beneficial aspects of H_2 pressure.

DISCUSSION

The results shown above demonstrate the wide-ranged ability of the model presented here. It is the only model to our knowledge that can calculate oil yields and evolution kinetics for an arbitrary temperature-pressure history. The model predicts decreased oil yield at lower heating rates and the maximum sensitivity to coke formation at 350°C. The model also predicts the delay of oil evolution and decreased oil yield at elevated pressures. The model also calculates the amount of unvaporized oil (bitumen) during the course of pyrolysis, although we have not attempted any comparisons to experiment.

The model does have some weaknesses. The calculated yields for Fischer Assay conditions and the Stout experiments (Figure 4) are systematically high by several percent. If we had limited our goal to modeling atmospheric pressure pyrolysis for heating rates of 720°C/h and lower, much better agreement could have been obtained. Instead, we adopted a maximum possible yield of 111% of the Fischer Assay value in order to account for rapid pyrolysis (3, 10) and high-pressure hydrogen experiments (11, 13) that obtain oil yields greater than Fischer Assay.

Another way of stating this problem is that the model overestimates the detrimental effect of pressure on oil yield, especially at slow heating rates. Because the calculated yield loss due to coking at slow heating rates does not increase much with increased pressure, the amount of oil cracking must be overestimated. We first attempted to solve this problem by not allowing liquid oil to crack, but a compensating increase in oil vapor cracking caused the oil yield to remain approximately constant. Since this paper was in draft form, we decided that the stoichiometry for oil cracking should be pressure dependent. Data of Voge and Good (22) indicate that the gas to light oil ratio of the cracking products decreases with increased pressure. Preliminary calculations using a pressure-dependent cracking stoichiometry indicate an improvement, but the model still overestimates the effect of heating rate at high pressure. This must be because the activation energy used for oil cracking is too low. It is also probably the reason why the cracking preexponential factor had to be reduced by a factor of 60 from that determined for shale oil between 500 and 650°C. Future work will explore the use of a higher activation energy.

Another apparent weakness is the calculation of too much hydrogen production at high pressure as shown in Table V. Increased H_2 production calculated by the model is due to oil coking and cracking. Our stoichiometry for these reactions was derived from atmospheric pressure experiments (6-8, 15). Apparently there are significant differences at higher pressures. One example of a difference is that alkenes are formed by oil cracking at atmospheric pressure, but none were formed from the cracking that occurred in the 2.7 Mpa, 1°C/h experiment, apparently because the hydrogen radicals are all captured by hydrocarbon radicals. Future work on model development will attempt to take this into account. The model also has a provision for reaction of H_2 with char to form methane, but its use has not yet been explored.

Although the model was designed to have the capability of allowing oil yields greater than obtained at Fischer Assay conditions, the model calculates nearly identical yields for pyrolysis at Fischer Assay conditions and for rapid pyrolysis in a sweep gas. Experiments indicate that the latter conditions give higher oil yields. Another weakness of the model for rapid pyrolysis involves hydrogen. Gas evolution kinetics have been reported by Richardson et al. (10) for isothermal fluidized-bed pyrolysis. They found that hydrogen (unlike other gases) did not reach its maximum rate of release until most of the oil was evolved, suggesting that it is formed by a reaction intermediate. In contrast, the model calculated that the maximum rate of hydrogen evolution was during the initial stages of kerogen pyrolysis, even though a major source of hydrogen is oil coking. A way to resolve this discrepancy is not yet apparent, but the problem emphasizes the importance of understanding the reactions of hydrogen for developing an improved general pyrolysis model.

A related problem is that the maximum possible oil yield is less than that attainable in high-pressure hydrogen. In the present model, the only way hydrogen can increase oil yield is by inhibiting oil coking. It appears necessary to include another mechanism in order to obtain higher yields in hydrogen than for flash pyrolysis. The recent ^{13}C NMR measurements of Herskowitz et al. (11) and Burnham and Happe (23) suggest how. High-pressure hydrogen appears to inhibit the formation of additional aromatic carbon during pyrolysis. Under a wide range of other conditions, the total amount of aromatic carbon in the oil and carbonaceous residue is roughly constant and nearly twice that present in the raw shale. These are important because our present model assumes that only part of the oil, roughly corresponding to the aromatic components, is susceptible to coking. Consequently, a higher fraction of the oil is likely to be susceptible to coking in the absence of added hydrogen donors. Therefore, it appears that the amount of oil susceptible to coking as well as the rate of coking should depend on hydrogen partial pressure.
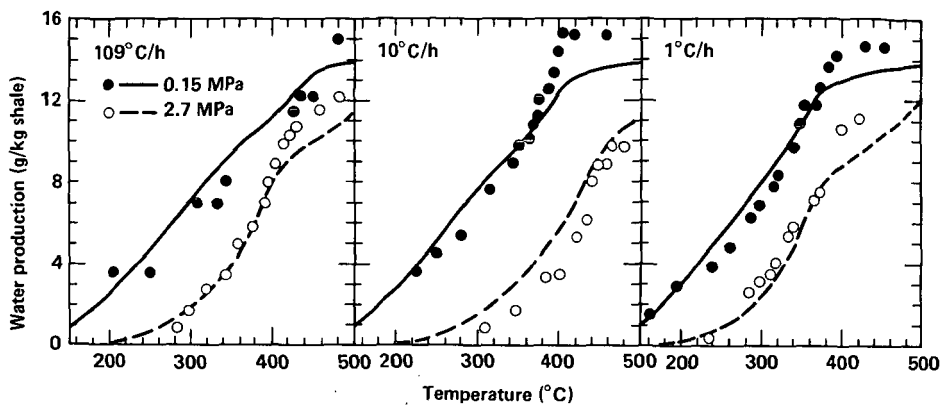
99

Figure 1. Comparison of calculated cumulative water production with measurements of Burnham and Singleton (12).
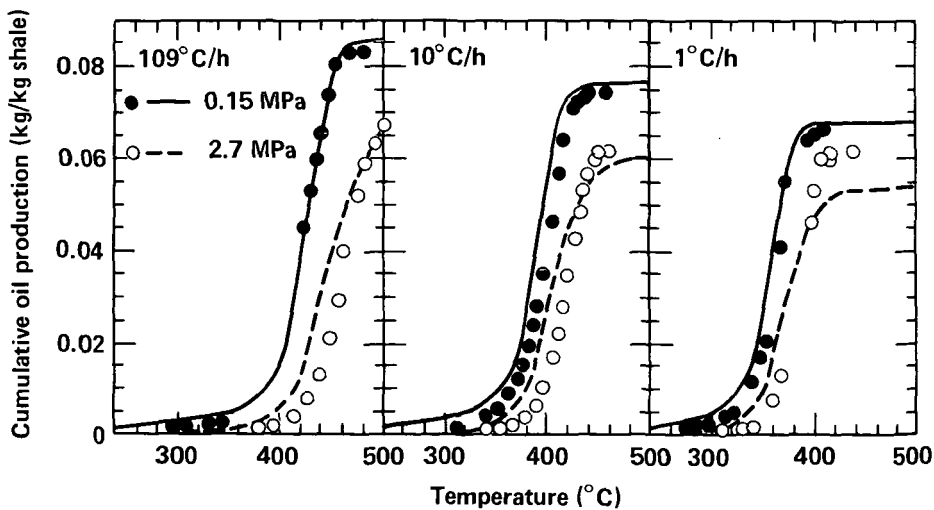

Figure 2. Comparison of calculated cumulative oil production with measurements of Burnham and Singleton (12).
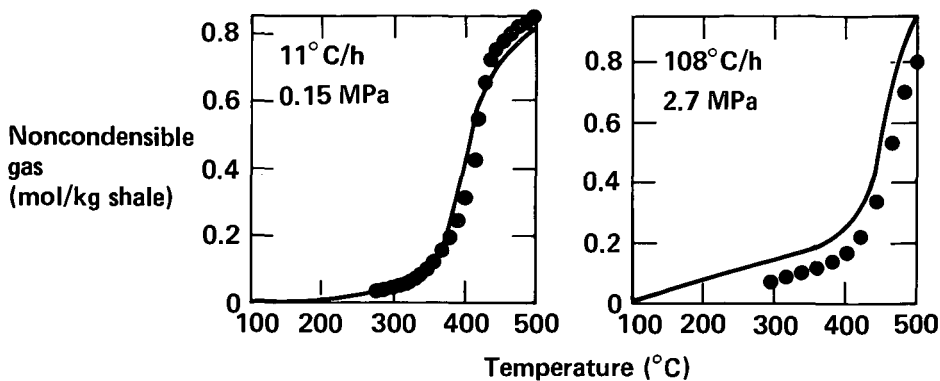
Figure 3. Comparison of calculated cumulative gas production with measurements of Burnham and Singleton (12).
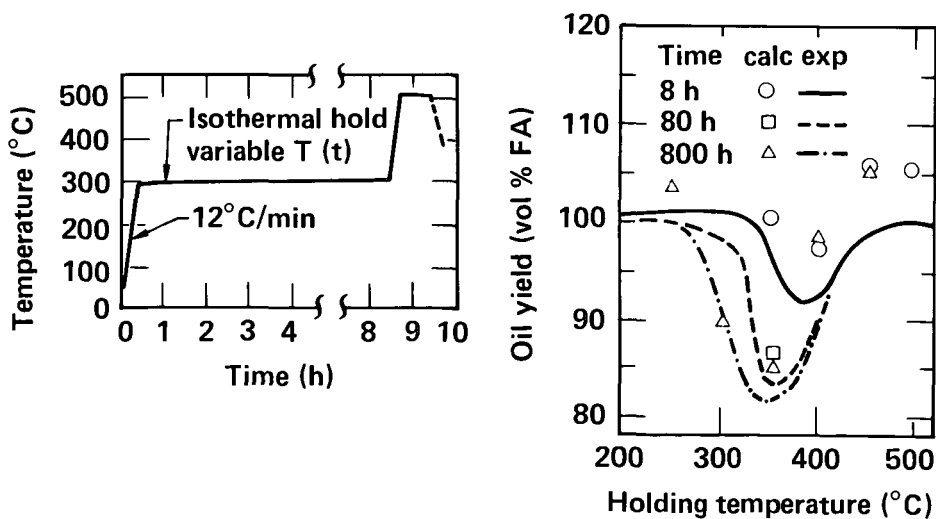

Figure 4. Thermal history of experiments by Stout et al. (6) and a comparison of calculated oil yields with their measurements.
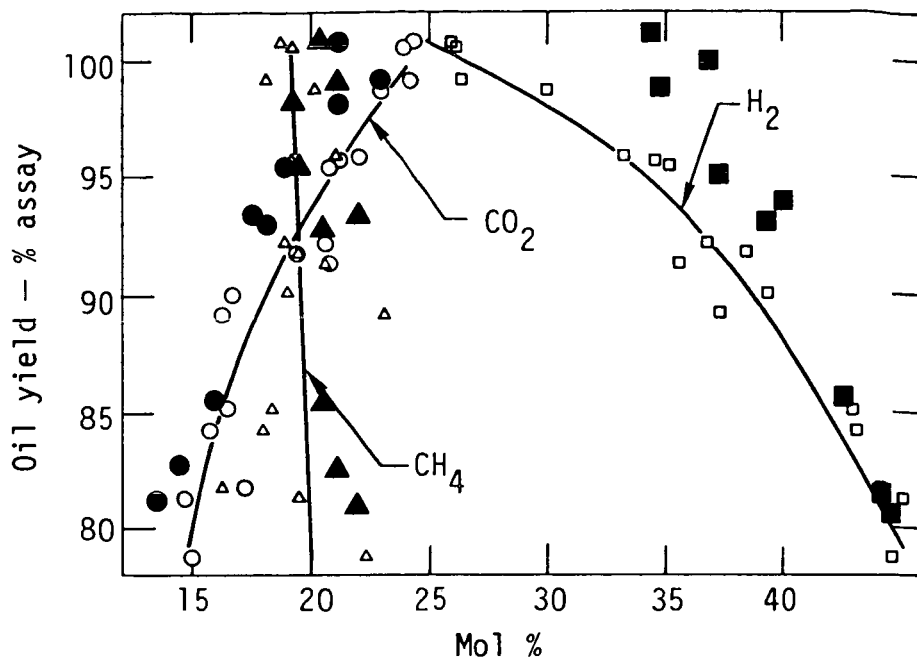
101

Figure 5. Comparison of calculated gas composition with results of Stout et al. (16).
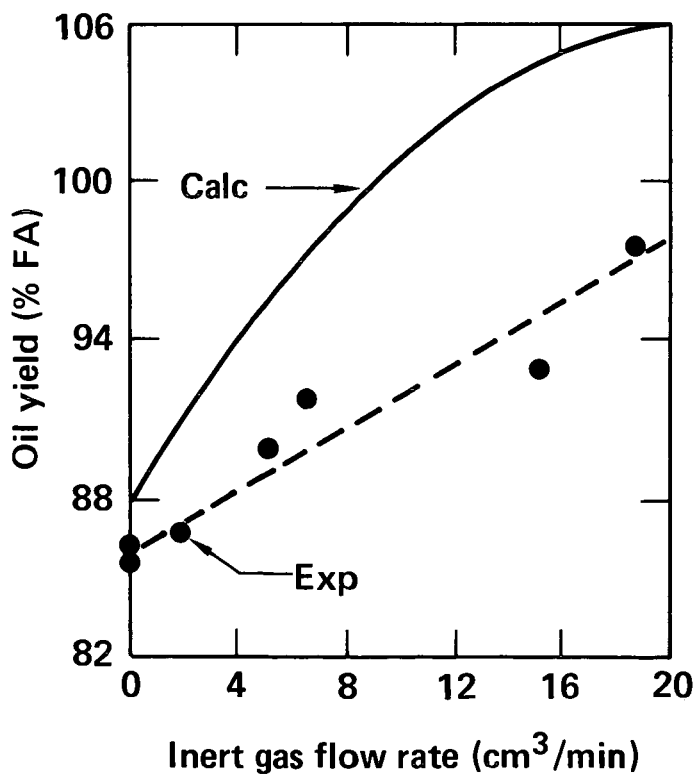

Figure 6. Comparison of calculated effect of flow rate with experiments of Campbell et al. (7).

LITERATURE CITED

(1)   Campbell, J. H., Koskinas, G. J. and Stout, N. D., Fuel, 57, 372 (1978).
(2)   Shih, S. M. and Sohn, H. Y., Ind. Eng. Chem. Proc. Des. Dev., 19, 420 (1980).
(3)   Wallman, P. H., Tamm, P. W. and Spars, B. G., "Oil Shale, Tar Sands and Related Materials", ACS Symp. Series No. 163, H. C. Stauffer, ed., Washington, D. C., p. 93 (1981).
(4)   Richardson, J. H., Huss, E. B., Ott, L. L., Clarkson, J. E., Bishop, M. O., Taylor, J. R., Gregory, L. J. and Morris, C. J., "Fluidized-bed Pyrolysis of Oil Shale: Oil Yield, Composition and Kinetics", Lawrence Livermore Natl. Lab. Rept. UCID-19548 (1982).
(5)   Braun, R. L. and Burnham, A. K., Oil Shale Project Quarterly Rept., Lawrence Livermore Natl. Lab. Rept. UCID-16986-82-2, p. 11 (1982).
(6)   Stout, N. D., Koskinas, G. J., Raley, J. H., Santor, S. D., Opila, R. L. and Rothman, A. J., Colo. Sch. Mines Quart., 71, 153 (1976).
(7)   Campbell, J. H., Koskinas, G. J., Stout, N. D. and Coburn, T. T., In Situ, 2, 1 (1978).
(8)   Burnham, A. K., "Oil Shale, Tar Sands and Related Materials", ACS Symp. Series No. 163, H. C. Stauffer, ed., Washington, D. C., p. 39 (1981).
(9)   Thakur, D. S., Vora, J. P., Wilkins, E. S. and Nuttall, H. E., Preprints, ACS, Div. Fuel Chem., 27 (2), 158 (1982).
(10)   Bissell, E. R., Burnham, A. K. and Braun, R. L., Lawrence Livermore Natl. Lab. Report UCRL-89976, submitted to I and EC Proc. Des. Dev. (1983).
(11)   Herskowitz, F., Olmstead, W. N., Rhodes, R. P. and Rose, K. D., "Chemistry and Geochemistry of Oil Shale", ACS Symp. Series 230, F. P. Miknis, ed., Washington, D. C., p. 301 (1983).
(12)   Burnham, A. K. and Singleton, M. F., "Chemistry and Geochemistry of Oil Shale", ACS Symp. Series 230, F. P. Miknis, ed., Washington, D. C., p. 335 (1983).
(13)   Weil, S. A. and Rue, D. M., Synthetic Fuels from Oil Shale II: Symp. Papers, Inst. Gas Technol., Chicago, IL, p. 217 (1982).
(14)   Hindmarsh, A. C., ACM SIGNUM Newsletter, 15 (4), 10 (1980).
(15)   Campbell, J. H., Gallegos, G. and Gregg, M., Fuel, 59, 727 (1980).
(16)   Huss, E. B. and Burnham, A. K., Fuel, 61, 1188 (1982).
(17)   Anthony, D. B. and Howard, J. B., AICHE J., 22, 725 (1976).
(18)   Singleton, M. F., Koskinas, G. J., Burnham, A. K. and Raley, J. H., "Assay Products from Green River Oil Shale", Lawrence Livermore Natl. Lab. Rept. UCRL-53273 (1982).
(19)   Voge, H. H. and Good, G. M., J. Am. Chem. Soc., 71, 593 (1949).
(20)   Fabuss, B. M., Smith, J. O. and Satterfield, C. N., Advances in Petroleum Chem. and Refining, 9, 157 (1964).
(21)   Brindley, G. W., Sharp, J. H., Patterson, J. H. and Narahari, B. N., Amer. Min., 52, 201 (1967).
(22)   Stone, R. L. and Rowland, R. A., Clays and Clay Minerals, Proc. 3rd Nat. Conf., p. 103 (1955).
(23)   Burnham, A. K. and Happe, J. A., Lawrence Livermore Natl. Lab., Report UCRL-89977, submitted to Fuel (1983).